RESEARCH ARTICLE

Analysis of electroencephalogram signals of depressed patients based on multi-dimensional features

Qinan Zhu[1, *], Zepeng Li[1], Yun Ke[2]

[1]College of Art and Design, Guangzhou Institute of Science and Technology, Guangzhou, Guangdong, China. [2]School of Arts and Media, Wuhan College, Wuhan, Hubei, China.

Received: October 13, 2025; **accepted:** February 5, 2026.

Electroencephalogram (EEG) offers a potential objective approach for depression diagnosis. However, existing methods often rely on single-dimensional features and small, noisy datasets, which limit diagnostic accuracy and generalizability. Moreover, due to the high dimension, nonlinearity, and low signal-to-noise ratio of EEG data, accurately diagnosing major depressive disorder through EEG signals remains a challenge. To solve these problems, this study extracted the global EEG features of depression EEG and combined the multi-dimensional EEG features with the generative adversarial network to realize the accurate diagnosis of major depression. The results showed that the Pearson correlation coefficients of all EEG features were in the range of -0.1 to 0.1. In the independent sample t-test results of C0 complexity, Coriolis complexity, and Shannon entropy, the *P* value of Levin variance equality test was greater than 0.05 and the mean equivalence T-test was less than 0.05. The average accuracy and F1 score of the proposed model were 0.9636 and 0.9620, respectively. This study provided an objective combination of biomarkers for depression identification and early intervention through electroencephalograph-based diagnosis.

Keywords: electroencephalogram; depression; generate adversarial network; multidimensional features.

***Corresponding author:** Qinan Zhu, College of Art and Design, Guangzhou Institute of Science and Technology, Guangzhou, Guangdong 510540, China. Email: paperxrk@163.com.

Introduction

Depression is a widespread mental disorder. Currently, its diagnosis relies heavily on subjective clinical assessments and self-reported scales, which can lead to inaccuracies and variability [1]. Electroencephalogram (EEG) reflects the electrical activity of nerve cells in the cerebral cortex or on the surface of the scalp, which makes it a promising objective approach for capturing neurophysiological changes associated with depression. EEG contains a large amount of physiological and disease-related information. It not only serves as the basis for diagnosing various brain diseases but also to monitor the therapeutic effect and has been widely applied in clinical medicine [2]. Studies have shown that patients with depression have significant changes in brain structure and function, and their EEGs contain multiple depression-related biomarkers, enabling the study of brain function and potential mechanisms [3, 4]. However, during the acquisition process, the quality of EEG signals is often affected due to the influence of environmental, equipment, and physiological factors. Therefore, preprocessing techniques are needed to filter out noise and artifacts, improve the signal-to-noise ratio, and ensure the accuracy of subsequent analysis. In recent years, various EEG-based methods for recognizing depression have been explored, which included multimodal fusion technology, extraction of geometric features from signal representations, and development of wearable sensing systems for inconspicuous data acquisition [5]. In addition, analyzing functional brain network dynamics and applying deep learning models such as convolutional and recurrent neural networks has demonstrated the potential to improve classification performance [6]. Supplementary studies on more extensive EEG analyses have also demonstrated the effectiveness of feature fusion strategies in enhancing the recognition of complex neural patterns in related neurological and mental disorders [7]. However, the key challenge remains. Most methods rely on one-dimensional features and ignore the nonlinear spatiotemporal dynamics of depression. Additionally, existing models are often overfit due to small clinical EEG samples and high noise levels.

Cai *et al*. developed a pervasive objective depression recognition system based on a multimodal fusion approach. The EEG data in three different modes were fused by using a feature level information fusion technique with well flexibility and depression recognition [8]. Akbari *et al*. obtained various geometric features of EEG using second order differential maps and then selected the most appropriate features by binary particle swarm algorithm. It ultimately achieved an average classification accuracy of 98.79% [9]. Tian *et al*. further designed a wearable three-lead EEG sensor to accurately acquire EEG data from the prefrontal lobe and extract its linear and nonlinear features. By using the ant lion optimization algorithm to weigh and choose the features, the method produced a high classification accuracy of 81.79% with a sensitivity of 81.79% [10]. Lin *et al*. obtained the region of interest of EEG signals (EEGS) in depressed patients by source localization and constructed a functional connectivity network based on it. The method used a sliding window approach and K-means clustering to examine dynamic connectivity and found that patients with depression were in sparsely connected states for longer periods of time and that their functional connectivity networks were less flexible than those of healthy subjects. The complexity and diversity of EEG in depressed patients made most of the computer-aided diagnostic strategies inaccurate [11]. Thoduparambil *et al*. used convolutional neural networks (CNN) and long short-term memory network (LSTM) to learn EEGS sequences and local features, respectively, with the accuracy of right hemisphere and left hemisphere EEGS as 99.07% and 98.84%, respectively [12]. The ability to extract useful features from the original EEGS is essential to EEGS analysis. To make the most of the rich and complex data found in the EEGS, researchers have studied EEGS feature fusion and categorization. Du *et al*. proposed a multi-feature fusion algorithm for motion imagery EEGS based on uniform flow shape approximation projection. The method fused the extracted multidomain features to generate low-dimensional features and then applied a k-nearest neighbor classifier in the low-dimensional space, which ultimately achieved an average accuracy of more than 92% [13]. Kang *et al*. objectively distinguished low-functioning autistic children by fusing multiple features utilizing the tenfold crossover to verify the accuracy of the model [14]. Priyasad *et al*. performed attention-driven data fusion of patient's EEG data through deep learning to achieve accurate assessment of epilepsy type with an F1 score of 0.967 [15]. Li *et al*. also applied a multi-feature fusion approach to EEGS classification of stroke patients to objectively and accurately realize the classification of electroencephalographic topography [16]. Kakkos *et al*. introduced a data-driven analysis framework that overcame the challenges of using fused EEG spectral features for task-independent load assessment and ultimately achieved a classification accuracy of 0.94 [17].

Existing studies on the diagnosis of depression EEG signals have limited feature extraction to single dimensional analysis, which is in the time or frequency domain and ignores the spatiotemporal nonlinear dynamic characteristics of EEG signals including functional connectivity flexibility and make it difficult to comprehensively characterize the multi-brain area coordination disorders of depression. Traditional deep learning models are limited by small sample data and high noise interference, which can lead to overfitting. Additionally, generative adversarial network (GAN) often uses fully connected layers to generate single channel spectra, resulting in the loss of temporal correlations in multi-channel EEG. To overcome the overfitting and insufficient generalization ability of existing deep learning models due to data scarcity, this research proposed a robust GAN-based EEG depression diagnosis model, Wasserstein GAN-DC (WGAN-DC), using small samples and high-noise clinical EEG data to extract pathological specificity from nonlinear, multidimensional EEG features. This research provided an interpretable combination of biomarkers and a new framework for the objective diagnosis of depression, supporting potential applications in clinical and resource-limited settings.

Materials and methods

Extraction of EEG features in depressed patients

The original EEGS was first processed using a SciPy Butterworth bandstop filter (NumFOCUS, Inc., Austin, TX, USA) and confirmed by using power spectral density (PSD) plot after noise removal. In digital signal processing, the sampling rate indicated the interval from a continuous signal to a discrete signal. The downsampling technique effectively reduced noise interference in EEGs while lowering the sampling rate and reducing the amount of data, thereby improving computational efficiency and saving memory. The study proposed to reduce the sampling rate of the EEGS from 250 Hz to 125 Hz and set the sampling time to 8 min. However, the acquired EEGS needed to be segmented into EEGSs with a period of 30 s for the segmentation processing of the acquired EEGS. The feature extraction process included signal preprocessing and examination of multiple microstate features including Kolmogorov-Chaitin complexity (KC), C0 complexity, Shannon entropy, PSD, which made it possible to characterize the EEGS in multiple dimensions and facilitated the effective extraction of features relevant to depression. The regularity, unpredictability, and complexity of EEG activity were described in neuroscience using a variety of complexity measures including KC [18]. KC was the length of the shortest computer program required to describe a string and was used to quantify the inherent complexity of the data. For any string s, there existed at least one description. If the length of the description $d(s)$ of s was minimized, it was called the "minimum description" of s. Meanwhile, the length of $d(s)$ was the length of the program that described the string. The length of $d(s)$ was the KC of s and was expressed as $K(s)$ below.

$$K(s) = |d(s)| \tag{1}$$

where a string was uncomplicated if it could be generated by a very short program $d(s)$. On the other hand, if generating a string required a longer program, then the string was considered complex. C0-complexity (C0) described the irregularity of the time series. The inverse Fourier transform (FT) was employed to derive a novel time series, and the C0 was derived by differencing the new time series and utilizing the sum of the squares of the differences to represent the value of the entire random component. The sum of the squares of the original time series was compared with the value of the random component. The degree of the known time series $\{f(k),\ k = 1,2,\dots,N-1\}$ of length $N-1$ was discrete Fourier transform (DFT) as foolows.

$$F_N(j) = \frac{1}{N}\sum_{k=0}^{N-1} f(k)e^{-2\pi i(kj/N)} \quad j = 0,1,2,\mathrm{K}\ ,N-1 \tag{2}$$

where $f(k)$ was a known discrete time series. $F_N(j)$ was the DFT result of time series $f(k)$. k was the time index of the original time series. j

was the frequency index of the transformed frequency-domain signal. The mean square value of $|F_N(j),\ j=0,2,\dots,N-1|$ was then calculated below.

$$G_N=\frac{1}{N}\sum_{j=0}^{N-1}\left|F_N(j)\right|^2 \tag{3}$$

where G_N was the mean square value of $F_N(j)$. The parameter r was introduced. The mean square r was retained by multiplying the spectrum and setting the rest to 0 as follows.

$$\tilde{F}_N(j)=\begin{cases}F_N(j),\ |F_N(j)|^2>rG_N\\0,\ |F_N(j)|^2\le rG_N\end{cases} \tag{4}$$

where r was greater than 1 and a given positive constant. A Fourier inverse transformation of $\tilde{F}_N(j)$ yielded a time series $\tilde{f}(k)$ of regular components as below.

$$\tilde{f}(k)=\sum_{j=0}^{N-1}\tilde{F}_N(j)e^{-2\pi i(kj/N)}\ j=0,1,2,\dots,N-1 \tag{5}$$

The final C0 expression was then obtained below.

$$C0(r)=\frac{\sum_{k=0}^{N-1}\left|f(k)-\tilde{f}(k)\right|^2}{\sum_{k=0}^{N-1}|f(k)|^2} \tag{6}$$

When r was equal to 1, $C0(r)$ was C0 as originally defined. The higher C0 represented the higher degree of irregularity of the time series, and vice versa the lower degree of irregularity. Shannon entropy characterized the magnitude of the amount of information and was calculated as follows.

$$H(X)=-\sum_{i=1}^{n}p(x_i)\,log_2\,p\,(x_i) \tag{7}$$

where $H(X)$ was the Shannon entropy of the continuous time series signal X. $p(x_i)$ was the probability that X took x_i. Shannon entropy was used to measure the uncertainty of a random variable. If the chance of a random variable was one, its entropy would be zero. This method was used to measure the complexity and uncertainty of the EEGS, as well as the functional connectivity of brain regions within the brain. PSD, a density function, was used to characterize a signal's frequency domain distribution. The method split the EEGS into multiple frequency components and then found the power spectrum of each component to observe the variation of the EEGS in different frequency bands and its correlation with cognition and behavior. For a continuous EEGS $x(t)$, its PSD $S_x(f)$ could be defined as the modulus square of the FT of the signal expressed below.

$$\begin{cases}X(f)=\int_{-\infty}^{+\infty}x(t)e^{-j2\pi ft}dt\\S_x(f)=|X(f)|^2\end{cases} \tag{8}$$

where $X(f)$ was the FT of $x(t)$. $|X(f)|$ was the magnitude of $X(f)$.

Recognition of depression based on multidimensional EEG features

The proposed WGAN-DC model used a conditional generator based on LSTM networks to synthesize realistic, multi-channel EEG signal time series and a joint discriminant classifier to evaluate signal authenticity and predict diagnostic categories simultaneously. If the original GAN was to facilitate the simultaneous advancement of generators and discriminators through adversarial learning, it was essential to ensure that the generators and discriminators were of equivalent strength. However, in the optimization process, there were instances where the generator was trained at a faster rate than the discriminator or vice versa, which could result in the generator outperforming the discriminator or vice versa, leading to training failure. In practice, however, it was often the explicitly labeled discriminators that underwent training at a faster pace. WGAN proposed an update suppression that suppressed the extent of each update to the network to a fixed range and was calculated as follows in place of the JS scatter.

$$W\left(P_r,P_g\right)=\inf_{\gamma:\prod\left(P_r,P_g\right)}E_{(x,y):\,\gamma}\left[\|x-y\|\right] \tag{9}$$

where P_r and P_g were the real and generated data distributions, respectively. $\gamma(x, y)$ was the joint distribution of P_r and P_g. The whole equation described the similarity of the distributions of P_r and P_g. However, since the joint distribution of γ was difficult to solve, an equivalent transformation was performed as below.

$$W\left(P_r, P_g\right) = \frac{1}{K} \sup_{\|f\|_L \leq K} E_{x: P_r}\left[f(x)\right] - E_{x: P_g}\left[f(x)\right] \quad (10)$$

where K was the Lipschitz constant to guarantee the function $f(x)$ satisfying the following equation and inscribed the maximum derivative of $f(x)$. f was the set of functions with gradient constraints. The WGAN-DC model was capable of classifying EEGSs in addition to generating multi-channel EEGS time series. The network integrated a conditional generator, a joint discriminator-classifier, and employed LSTM networks to preserve temporal correlations. The generator of the WGAN-DC model generated samples x_f conditional on the class label y in addition to generating random samples. The discriminator network of the original GAN model was then replaced with a joint discriminator-classifier network, which gave model the ability to perform supervised learning from training data with class label y_r. The discriminators and classifiers shared the lower layers of the network with parameters and split into two branches at the output as the discriminator branch D with parameter ϕ_D and the classifier branch ϕ_C with parameter ϕ_S. The WGAN-DC model trained the classifiers as part of the GAN, taking full advantage of the GAN's ability to learn data representations and improving the classification performance of the classifiers while generating EEGSs. Decision quantity $Decision(i, j) \geq m \times r$ was constructed as a sufficient condition for determining that the vectors $X_i^{(m)}$ and $X_j^{(m)}$ had non-similarity with its specific mathematical definition as follows.

$$Decision(i, j) = \left|\sum_{k=0}^{m-1} x_{i+k} - \sum_{k=0}^{m-1} x_{k+k}\right| \geq m \times r \quad (11)$$

where m was the embedding dimension of the entropy measure computing parameter. The similarity tolerance of the entropy measure calculation parameters was indicated by r. In the context of estimating approximate entropy and sample entropy, any two m-dimensional vectors $X_i^{(m)}$ and $X_j^{(m)}$ that fell inside the r similarity tolerance were deemed comparable as below.

$$\begin{cases} \left|x_{i+k} - x_{j+k}\right| < r, \forall k, 0 \leq k \leq m-1 \\ \left|x_{i+k} - x_{j+k}\right| > r, \exists k, 0 \leq k \leq m-1 \end{cases} \quad (12)$$

When the decision quantity $Decision(i, j)$ satisfied condition $Decision(i, j) \geq m \times r$, the corresponding two vectors $X_i^{(m)}$ and $X_j^{(m)}$ were necessarily dissimilar. If the two m-dimensional vectors $X_i^{(m)}$ and $X_j^{(m)}$ were similar, the absolute value of the subtraction by subtracting their corresponding m components would necessarily be smaller than $m \times r$ as follows.

$$max\{\left|x_{i+k} - x_{j+k}\right|\} < r, 0 \leq k \leq m-1 \Rightarrow \sum_{k=0}^{m-1}\left|\left(x_{i+k} - x_{j+k}\right)\right| < m \times r \quad (13)$$

According to the mathematical definition of $Decision(i, j)$, Equation (14) was derived by knowing $Decision(i, j) \geq m \times r$.

$$\begin{cases} \left|\sum_{k=0}^{m-1} x_{i+k} - \sum_{k=0}^{m-1} x_{j+k}\right| \geq m \times r \\ \left|\sum_{k=0}^{m-1} x_{i+k} - \sum_{k=0}^{m-1} x_{j+k}\right| \geq m \times r \Leftrightarrow \left|\sum_{k=0}^{m-1}\left(x_{i+k} - x_{j+k}\right)\right| \geq m \times r \end{cases} \quad (14)$$

where the addition of the absolute values of the corresponding parts of the vectors $X_i^{(m)}$ and $X_j^{(m)}$, representing any two m dimensions, yielded a result larger than $m \times r$. Therefore, from equations (9) and (13), the vectors $X_i^{(m)}$ and $X_j^{(m)}$ were not similar because it was necessarily to follow the equation (15) below.

$$max\left\{\left|\left(x_{i+k} - x_{j+k}\right)\right|\right\} > r,\ 0 \le k \le m-1 \quad (15)$$

The sample entropy of the EEG data was sequentially extracted from the time window using a window width of t_w and moving along the time axis for Δt each time. The sample entropy expression with embedding dimension m and similarity threshold r was defined as $DySampEn(m,r)$. Thus, the dynamic sample entropy expression for an EEG time series with time length T was shown as follows.

$$DySampEn\left(m,r\right)_{\langle k\rangle} = SampEn\left(m,r\right)_{\langle k\rangle},\ 1 \le k \le W \quad (16)$$

LSTM was a sequence model often for sequence prediction and generation. Generators based on LSTM networks could maintain temporal correlation, have a more complex structure, and better learning performance than fully connected layers. To generate complex temporal sequence data of EEG, this study replaced the fully connected layer with LSTM. The network input shape of this generator was (None, 32, 16). It was first processed by the LSTM layer and output a sequence of (None, 32, 128). Then, it passed through the LeakyReLU activation function to keep the dimension unchanged. The data was then flattened into a one-dimensional vector of (None, 4,096), and dimension reconstruction was performed to obtain a feature map of (None, 2, 16, 128). Subsequently, the network gradually enhanced the spatial resolution of the feature map through a series of Upsampling operations to (None, 4, 32, 128) followed by undergoing Batch normalization and LeakyReLU activation before upsampling again to (None, 8, 64, 128). The batch normalization and activation were performed in the same way. The subsequent layers further transformed and refined the features through a combination of upsampling, convolution, batch normalization, and activation functions. The feature map was upsampled to (None, 384, 16) and then output through the convolutional layer to (None, 8, 64, 64). After batch normalization and activation, the feature map was converted to (None, 16, 128, 128) through the deconvolution layer. Batch normalization and activation were then carried out. The final generated EEG signal was output through a convolutional layer with the shape of (None, 16, 128, 1). This design ensured that the generator could effectively reconstruct a multi-channel EEG signal time series with a reasonable spatiotemporal structure from the latent representation. The constructed WGAN-DC model incorporated several key components to enhance its performance. Both generator and discriminator used a multi-head attention mechanism to increase their representational capacity. Generators were divided into encoders and decoders. The encoder was mainly composed of CNN and multi-head attention module. In each convolution layer, a convolution kernel with size of 128 × 1 and a convolution operation with step size of 2 were used. In addition, LeakyReLU was added after each convolutional layer as the activation function. The decoder was mainly composed of deconvolution layer and multi-head attention module. The study used a deconvolution kernel with a size of 128 × 1 and a deconvolution operation with a step size of 2 in the deconvolution layer. LeakyReLU was added as the activation function after each deconvolution layer. Concurrently, two residual connections were incorporated into the convolutional layer and the deconvolution layer, respectively, to enhance the preservation of the features inherent in the original EEG. The multi-head attention mechanism was used to control which regions in the EEG the generator focused on. By using the self-attention mechanism to calculate the weight of each pixel before weighing and summing the output feature map to ensure high-quality generated EEG signals. The input of the discriminator consisted of real EEG signals and synthetic EEG signals, which were composed of 3 fully connected layers. In the first two fully connected layers, LeakyReLU was used as the activation function to enhance the non-linear characteristics of the network. The final layer of the fully connected layer output the authenticity judgment of the input sample with “Real” as a real sample and “Fake” as a synthetic sample.

Recruitment and grouping of research subjects

Multimodal open dataset for mental disorder analysis (http://modma.lzu.edu.cn/data/index/) (MODMA) was employed in this research, which contained resting-state EEG data from patients with major depressive disorder (DG) and healthy controls (HG). The DG group included 40 patients (20 males and 20 females), aged from 25 - 52 years old with average age of 38.62 ± 6.74 years old. All patients were diagnosed by psychiatrists in accordance with the criteria of diagnostic and statistical manual of mental disorders (DSM-5) and were mainly recruited from Lanzhou Mental Health Center (Lanzhou, Gansu, China). The HG group included 40 participants (19 males and 21 females), aged from 20 - 41 years old with an average age of 27.41 ± 7.63 years old. All subjects in the health control group were confirmed without history of mental or severe neurological diseases through general physical examinations and were recruited through advertisements on the campus of Lanzhou University (Lanzhou, Gansu, China) and the surrounding communities. The procedures of this research were approved by the Academic Ethics Committee of Wuhan University (Wuhan, Hubei, China). All participants signed the informed consent form before participating.

EEG data collection

EEG data was collected using ANT Neuro's 128-lead WaveGuard EEG system (ANT Neuro B.V., Enschede, The Netherlands). According to the MODMA, data from 19 standard leads that conformed to the international 10 - 20 system were selected. The data were collected during subject resting time with their eyes closed at a sampling rate of 250 Hz and the recording duration of 5 minutes.

Model validation

Model validation adopted a strict data partitioning and performance evaluation process. For the 80 subjects in the MODMA dataset, 5-fold stratified cross-validation was adopted. In each compromise, the data were randomly divided by subject level into a training set (64 subjects, accounting for 80%), a validation set (8 subjects, accounting for 10%), and a test set (8 subjects, accounting for 10%) with completely invisible throughout the process.

Computational environment

The proposed WGAN-DC model was run in Python v3.7 (Python Software Foundation, Wilmington, DE, USA), PyTorch v1.10 (Meta Platforms, Inc., Menlo Park, CA, USA), and CUDA v11.4 (NVIDIA Corporation, Santa Clara, CA, USA) environments with GeForce GTX 1080Ti GPU (NVIDIA Corporation, Santa Clara, CA, USA). The RMSprop optimizer implemented in PyTorch's torch.optim module was used to train the generator and discriminator with a total of 120 training cycles and the learning rates of 0.0001. The mask probability was set to 0.3 and the number of heads in the multi-head attention mechanism was set to 4.

Evaluation of proposed model

Two classic deep learning baseline models including classic CNN architecture and bidirectional long short-term memory (BiLSTM) network were employed for comparison study with proposed WGAN-DC model. The classic CNN architecture was for EEG classification [19], while BiLSTM network was for sequential data modeling [20]. All models were partitioned using the same training/validation/test data. Five general indicators for calculation and comparison were adopted to comprehensively and quantitatively evaluate the classification performance of the proposed model and the baseline model. All indicators were defined based on the confusion matrix in the binary classification task, where the "depression patients" sample was labeled as the positive category. Accuracy measured the proportion of models that made correct predictions in all samples and was calculated as follows.

$$\text{Accuracy} = \frac{TP + TN}{TP + TN + FP + FN} \tag{17}$$

where TP (true positive) and TN (true negative) were the numbers of correctly predicted positive and negative samples, respectively. FP (false positive) was the number of negative class samples that were mistakenly predicted as positive class samples. FN (false negative) was the number of positive class samples that were wrongly predicted as negative class samples. The recall rate measured the proportion of samples that were actually positive classes and correctly predicted by the model, which focused on the model's ability to recognize positive classes and was calculated below.

$$\text{Recall} = \frac{TP}{TP + FN} \tag{18}$$

The F1 score was the harmonic mean of precision and recall and was used to evaluate the model's performance comprehensively with the calculation as follows.

$$F_1 = 2 \times \frac{\text{Precision} \times \text{Recall}}{\text{Precision} + \text{Recall}} \tag{19}$$

The area under the receiver operating characteristic (ROC) curve (AUC) measured the model's ability to distinguish between positive and negative class samples. The closer the AUC value was to 1.0, the better the model's classification performance. An AUC value of 0.5 indicated that the performance was equivalent to random guessing. The ROC curve was plotted with the false positive rate (FPR) as the horizontal axis and the true positive rate (TPR) as the vertical axis by changing the classification threshold and were calculated below.

$$\begin{cases} \text{TPR} = \dfrac{TP}{TP + FN} \\ \text{FPR} = \dfrac{FP}{FP + TN} \end{cases} \tag{20}$$

Statistical analysis

All statistical analyses in this study were conducted using SPSS v. 26.0 software (IBM, Armonk, NY, USA). Independent sample t-tests were conducted to compare the differences in multi-dimensional EEG features between DG and HG groups on the mean values of each channel feature in each group. Levene tests were pre-performed to evaluate homogeneity of variance. The linear correlation between features was evaluated by calculating the Pearson correlation coefficient (PCC). P values less than 0.05 were defined as statistically significant.

Results and discussion

Global EEG features

The comparison results of the mean values of four multi-dimensional EEG features in 19 channels between DG and HG demonstrated that C0 MV of most channels in DG was consistently higher than that in HG (Figure 1a), which indicated that patients with depression had EEGs with higher irregularity. The average values of each channel in DG were lower for KC compared with HG (Figure 1b), indicating a reduction in the complexity of neural signals in depression. The MV of PSD showed some differences among different channel groups, but there was no consistent dominant trend (Figure 1c). The average value of Shannon entropy in DG was generally lower than that in HG (Figure 1d), which reflected a reduction in the complexity or amount of information in the EEG signals of patients with depression. These observations collectively indicated that depression was associated with problems of low complexity, high irregularity, low information entropy, and potential changes in band power. By analyzing the MV of each channel in the entire brain EEGS, the average horizontal violin plot of the global EEGS was obtained and showed that the C0 in DG demonstrated a higher median and a more compact data distribution with narrower violin shape than HG, which confirmed the increased irregularity of EEG in patients with depression (Figure 2a). A lower median and a wider distribution (wider violin) were observed in DG, indicating a decrease in signal complexity and greater variability (Figure 2b). Regarding the PSD, the violin plots of the two groups overlapped significantly, indicating similar medians and distributions, which suggested that there were no significant overall differences in alpha power

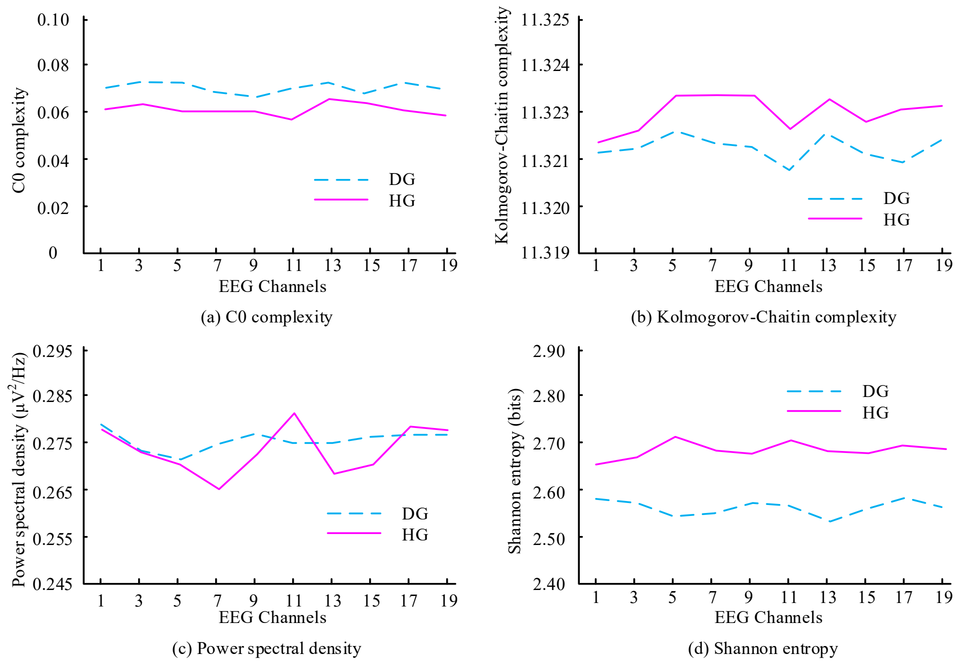

Figure 1. Comparison of channels' mean values of global EEG features.

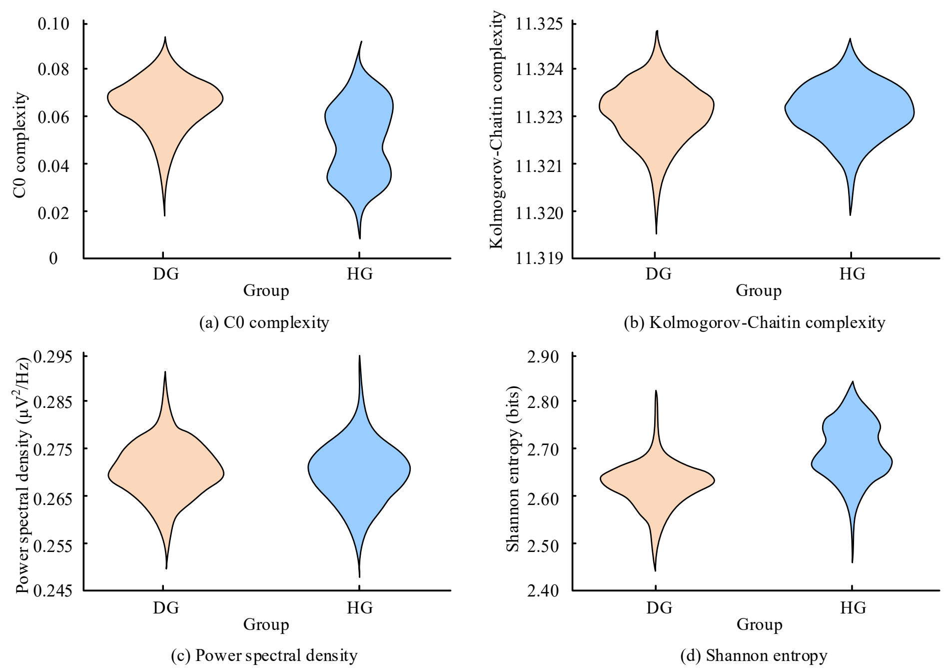

Figure 2. Distribution of global EEG features over DG and HG.

at this level (Figure 2c). For the Shannon entropy, DG's distribution shifted downward, showing a lower median and dense concentrations of lower values, which reflected an overall decrease in information content (Figure 2d).

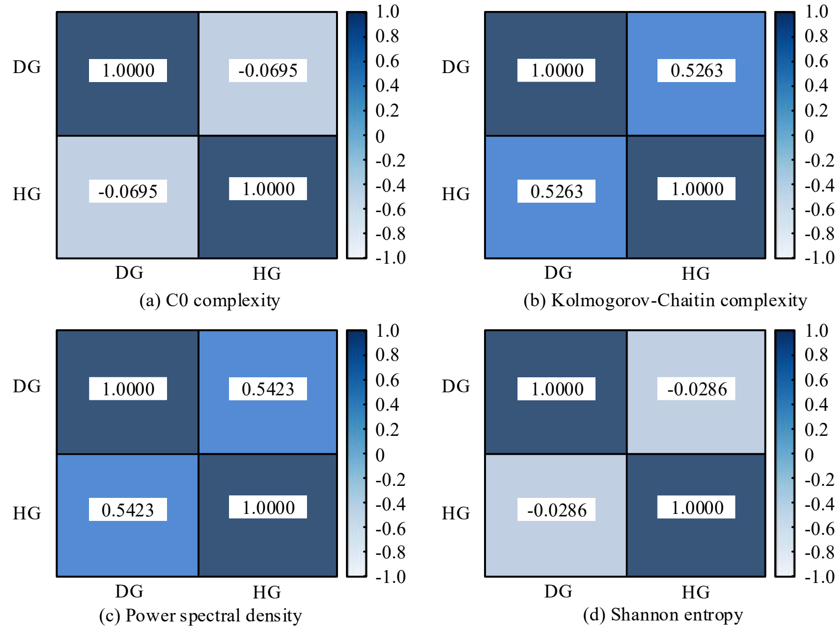

Figure 3. Correlation of mean value of each channel between DG group and HG group under different characteristics.

Relationship between mean levels of individual channels in the two groups

The results showed that the PCC values were negative for C0 complexity and PSD characteristics, and the mean changes between DG and HG on these characteristics were in the opposite direction. However, the trend of the mean change in KC and Shannon entropy was the same, which indicated that the trend of the mean change in the two characteristics of DG and HG was the same. The PCC values of each index were from -0.1 to 0.1, indicating a weak linear relationship between the mean levels of EEG activities of the two groups. In addition, the correlation coefficient of C0 complexity and KC were -0.0695 and 0.05263, respectively, indicating the largest negative correlation (Figure 3). The channels' statistical analysis of DG and HG clusters with different overall EEG properties demonstrated that Levene's tests for C0, KC, and Shannon entropy all showed no significant differences, indicating homogeneity of variances, while the mean values between DG and HG showed significant difference ($P < 0.05$). In contrast, Levene's test showed significant difference in variances for PSD ($P < 0.05$), while the t-test for mean equality showed no significant difference, indicating a distinct statistical profile for PSD compared to the other features.

Analysis of depression identification outcomes

The study compared the dimensionality reduction properties of the augmented signals generated by different GANs and with the dimensionality reduction distribution of the original EEG by mapping the global EEGS into a two-dimensional space and obtaining its downscaled distribution. The fully connected layer produced many samples beyond the distribution of the original samples when the fully connected layer performed sample augmentation, and such samples might give wrong information to the depression discrimination model (Figure 4a). The data generated by LSTM was closer to the actual distribution of the EEG than the complete connectivity layer (Figure 4b). Moreover, LSTM could better portray the timing characteristics of the timing signal and its correlation, which made the obtained EEG more consistent with the distribution characteristics of the original EEG. The results suggested that the proposed algorithm could successfully compensate for the

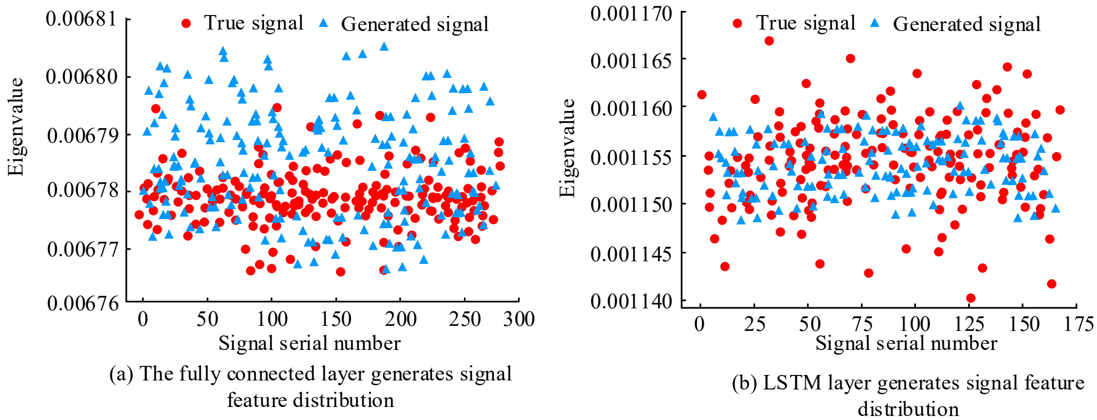

Figure 4. Generates the signal feature distribution.

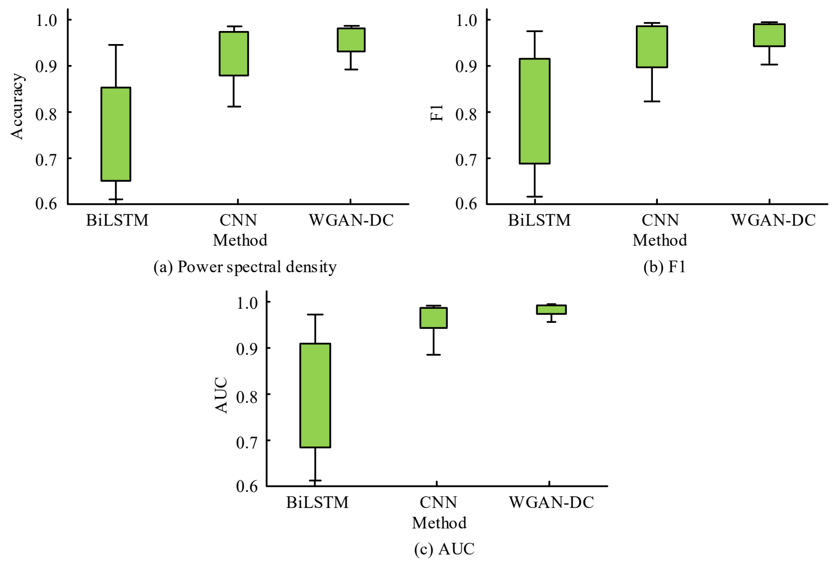

Figure 5. Comparison of models' specificity.

sample's shortcomings, offer more detailed information for the model's creation, and enhance the algorithm's overall effectiveness. The study used the same training and test samples for bidirectional LTSM network (BiLSTM) and CNN. The results showed that the best classification outcomes were obtained by using WGAN-DC algorithm with an average correctness of 0.9598 and an F1 score of 0.9731. The detection effect of proposed algorithm was better than that of CNN and BiLSTM with the prediction precision of WGAN-DC algorithm as 0.9672 and AUC as 0.9836, which were better than that of CNN and BiLSTM (Figure 5). The results indicated that WGAN-DC had better generalization and better stability. To verify the effectiveness of focus loss, the study examined the proposed WGAN-DC, BiLSTM, and CNN models and compared the classification results of different models on different datasets. In general, the model performance on the test set was better than the training set. In the training set, WGAN-DC model improved the classification accuracy by about 3% over the other two models. In the test set, WGAN-DC model outperformed BiLSTM and CNN models, improving the classification accuracy by about 5% (Figure 6).

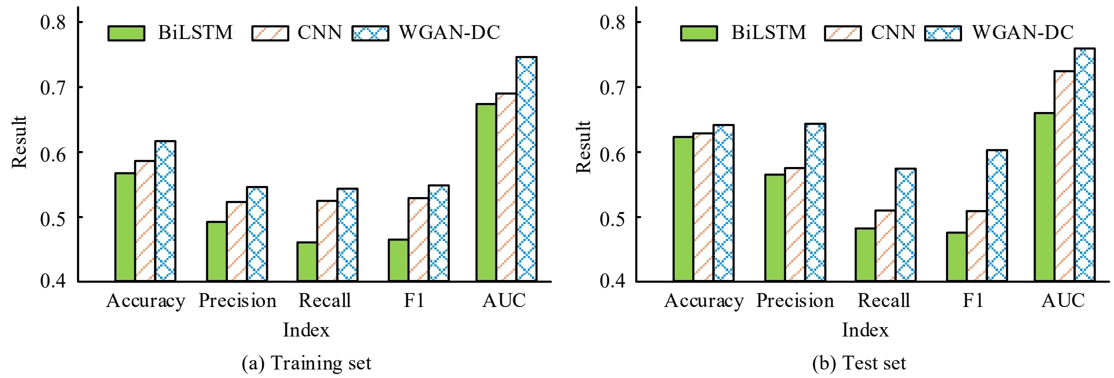

Figure 6. The results of categories imbalance.

Classifier training by WGAN-DC model

The results showed that WGAN-DC augmentation achieved accuracy, precision, recall, F1 score, and AUC as 0.574, 0.367, 0.392, 0.364, and 0.614, respectively, while CNN-based augmentation's accuracy, precision, recall, F1 score, and AUC were 0.587, 0.550, 0.532, 0.524, and 0.692, respectively, and BiLSTM-based augmentation showed the improved performance with the accuracy, precision, recall, F1 score, and AUC as 0.610, 0.529, 0.513, 0.517, and 0.715, respectively. Notably, the proposed WGAN-DC augmentation method achieved the highest overall discriminative performance. The results demonstrated that classifiers trained using WGAN-DC model outperformed those trained by using traditional augmentation methods in terms of balanced metrics, which indicated that WGAN-DC model had a superior ability to capture the underlying data distribution and enhanced classification robustness. The improved performance was largely attributed to the high-quality synthetic samples generated by WGAN-DC, which effectively augmented underrepresented data and refined the decision boundary.

The results of this research collectively indicated that the EEG of patients with depression presented a multi-dimensional pattern that featured low complexity with decreased KC, high irregularity with increased C0, and attenuation of information entropy with decreased Shannon entropy. This collaborative characteristic change provided a set of explainable biomarker combinations for the objective diagnosis of depression. Its classification performance was expected to be significantly better than that of a single feature through multi-dimensional feature fusion for collaborative discrimination and provided clinicians with a potential objective tool to quantify symptom severity in routine evaluations. In addition, time-varying features such as dynamic sample entropy were expected to provide real-time monitoring methods for treatment responses by tracking the temporal changes in neural complexity. Although the proposed WGAN-DC model performed well in the study, its reliance on high-quality EEG instrument might limit its application in scenarios with limited resources. To achieve real-time screening, the model's high computational complexity must be addressed. Future research should develop more interpretable methods for feature interaction analysis. Through model compression and edge computing technology, WGAN-DC was deployed to mobile terminals to achieve real-time depression screening.

Acknowledgements

The research was supported by 2025 Huizhou Philosophy and Social Sciences Planning Project (Grant No. HZSK2025GJ14), the Horizontal projects of Wuhan College (Grant No. H2024175), School Level Scientific Research Innovation Team of Wuhan College in 2020 (Grant No. kyt202001).

References

1. Usman AM, Abdullah MK. 2023. An assessment of building energy consumption characteristics using analytical energy and carbon footprint assessment model. Green Low-Carbon Econ. 1(1):28-40.
2. Aryavalli SNG, Kumar GH. 2023. Futuristic vigilance: Empowering chipko movement with cyber-savvy IoT to safeguard forests. Arch Adv Eng Sci. 1(8):1-16.
3. Cao H, Wu Y, Bao Y, Feng X, Wan S, Qian C. 2023. UTrans-Net: A model for short-term precipitation prediction. Artif Intell Appl. 1(2):106-113.
4. Huang JX, Hsieh CY, Huang YL, Wei CS. 2022. Toward CNN-based motor-imagery EEG classification with fuzzy fusion. Int J Fuzzy Syst. 24(8):3812-3823.
5. Goshvarpour A, Goshvarpour A. 2020. Schizophrenia diagnosis using innovative EEG feature-level fusion schemes. Phys Eng Sci Med. 43(1):227-238.
6. Liu K, Sun Y, Yang D. 2023. The administrative center or economic center: Which dominates the regional green development pattern. A case study of Shandong peninsula urban agglomeration, China. Green Low-Carbon Econ. 1(3):110-120.
7. Cichy RM, Oliva A. 2020. A M/EEG-fMRI fusion primer: Resolving human brain responses in space and time. Neuron. 107(5):772-781.
8. Cai H, Qu Z, Li Z, Zhang Y, Hu B. 2020. Feature-level fusion approaches based on multimodal EEG data for depression recognition. Inf Fusion. 59:127-138.
9. Akbari H, Sadiq MT, Payan M, Esmaili SS, Bagheri H. 2021. Depression detection based on geometrical features extracted from SODP shape of EEG signals and binary PSO. Trait Signal. 38(1):13-26.
10. Tian F, Zhu L, Shi QX, Wang R, Zhang L, Dong Q, *et al*. 2023. The three-lead EEG sensor: Introducing an EEG-assisted depression diagnosis system based on ant lion optimization. IEEE Trans Biomed Circuits Syst. 17(6):1305-1318.
11. Lin XB, Kong WZ, Li JX, Shao X, Jiang C, Yu R, *et al*. 2023. Aberrant static and dynamic functional brain network in depression based on EEG source localization. IEEE-ACM Trans Comput Biol Bioinform. 20(3):1876-1889.
12. Thoduparambil PP, Dominic A, Varghese SM. 2020. EEG-based deep learning model for the automatic detection of clinical depression. Phys Eng Sci Med. 43(4):1349-1360.
13. Du Y, Sui J, Wang S, Fu R, Jia C. 2023. Motor intent recognition of multi-feature fusion EEG signals by UMAP algorithm. Med Biol Eng Comput. 61(10):2665-2676.
14. Kang J, Jin Y, Liang G, Li X. 2021. Accurate assessment of low-function autistic children based on EEG feature fusion. J Clin Neurosci. 90:351-358.
15. Priyasad D, Fernando T, Denman S, Sridharan S, Fookes C. 2021. Interpretable seizure classification using unprocessed EEG with multi-channel attentive feature fusion. IEEE Sens J. 21(17):19186-19197.
16. Li F, Fan Y, Zhang X, Wang C, Hui H. 2020. Multi-feature fusion method based on EEG signal and its application in stroke classification. J Med Syst. 44(2):1-11.
17. Kakkos I, Dimitrakopoulos GN, Sun Y, Yuan JJ, Matsopoulos GK, Bezerianos A, *et al*. 2021. EEG fingerprints of task-independent mental workload discrimination. IEEE J Biomed Health Inform. 25(10):3824-3833.
18. Jindal K, Upadhyay R, Singh HS. 2024. A hybrid ensemble voting-based residual attention network for motor imagery EEG classification. Analog Integr Circ Sig Process. 119(1):165-184.
19. Yu D, Li P, Su F, Wang K, Duan S, Yuan D. 2025. Automatic detection of depression using a CNN-Transformer model based on low-channel EEG data. Turk J Electr Eng Comput Sci. 33(5):594-612.
20. Challapalli JR, Devarakonda N, Nandipati BL, Durgam R. 2025. Hybrid fine-tuned bert and deep learning classifiers for early detection and analysis of depression across diverse data modalities. Trait Signal. 42(5):2837-2851.